ELSEVIER

Materials Science and Engineering B 120 (2005) 16–20

MATERIALS SCIENCE & ENGINEERING B

www.elsevier.com/locate/mseb

Modeling of ferroelectric domains in thin films and superlattices

F. De Guerville[a], I. Luk'yanchuk[a,b,*], L. Lahoche[a], M. El Marssi[a]

[a] *University of Picardie Jules Verne, LPMC-UPJV, 33 rue St. Leu, 80039 Amiens, France*
[b] *L.D. Landau Institute for Theoretical Physics, Moscow, Russia*

Abstract

We have developed the set of numerical (finite-element) and analytical tools that are based on the self-consistent solution of the electrostatic equations coupled with material Ginzburg–Landau equations with an objective to model the profile of domain textures in the entire temperature region. We calculated the evolution of principal parameters of domain texture: modulation vector, distribution of polarization, renormalization of critical temperature etc. In contrast to the Kittel approximation we conclude that the profile of polarization across domains in nanometric ferroelectric thin films is highly nonuniform.
© 2005 Elsevier B.V. All rights reserved.

Keywords: Ferroelectric domains; Thin films; Superlattices; Modeling

1. Introduction

Ferroelectric polarization domains are created in ferroelectric slabs and films to reduce the energy of the depolarization field produced by the space and surface charges with charge density $\rho(r) = \mathrm{div}\,\mathbf{P}$ that are provided by the discontinuity and nonuniformity of the polarization close to the crystal surface. Usually, the domain formation is considered in the so-called Kittel approximation [1–3] when the polarization is assumed to have the uniform flat profile across domains. Being valid at low temperatures, this approximation does not allow to analyze neither the temperature evolution of domain texture nor the influence of the surface and interface phenomena. Meanwhile these effects play the decisive role in thermodynamic and electric properties of the emerging nanoscopic ferroelectric devices.

In this communication we present the results of more complete study of ferroelectric domains and domain textures based on the self-consistent solution of the coupled electrostatic and Ginzburg–Landau equations for two mathematically equivalent geometries, shown in Fig. 1:

(a) For ferroelectric thin film of nanometric thickness $2a_f$ surrounded by paraelectric passive layers of thickness a_p and embedded in a short circuited capacitor.
(b) For a periodic superlattice structure consisting of alternate ferroelectric and paraelectric layers of nanometric thickness $2a_f$ and $2a_p$.

For numerical solution of these equations we developed the finite-element PDE tool-box that allows to work over the entire temperature interval and for a wide region of sample parameters. The consistency of numerical results with approximate solution at low temperatures (Kittel approximation) [1–3] and in the vicinity of transition temperature T_c [4,5] was controlled.

Our principal result is that, two shown in Fig. 2 types of domain structures can exist in thin films and superlattices. *Soft domains* (a) with gradual polarization profile that occur close to transition temperature T_c and in thin nanometric films and *hard domains* (b) with flat Kittel-like polarization profile that are realized at low temperatures and in thick ferroelectric films. These structures have the different physical properties that are discussed in the communication.

We restrict ourself to the case of suitable for application displacive high-ε ferroelectric materials. Only 180° z-oriented domains are considered. To avoid the complications of the effect of 90° ferroelastic domains (like in a cubic per-

* Corresponding author. Fax: +33 3 22 82 78 91.
E-mail address: lukyanc@ferroix.net (I. Luk'yanchuk).

0921-5107/$ – see front matter © 2005 Elsevier B.V. All rights reserved.
doi:10.1016/j.mseb.2005.02.039

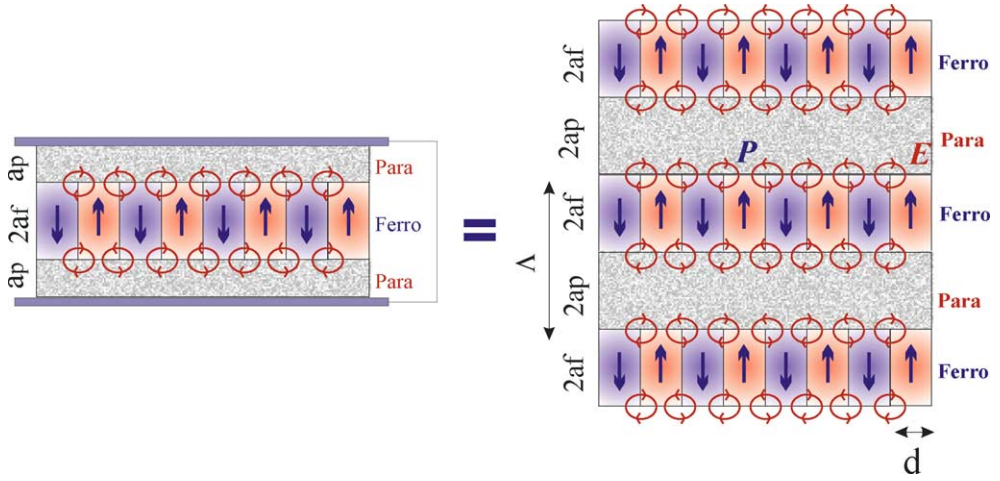

Fig. 1. Capacitor- and superlattice-like geometry of the problem.

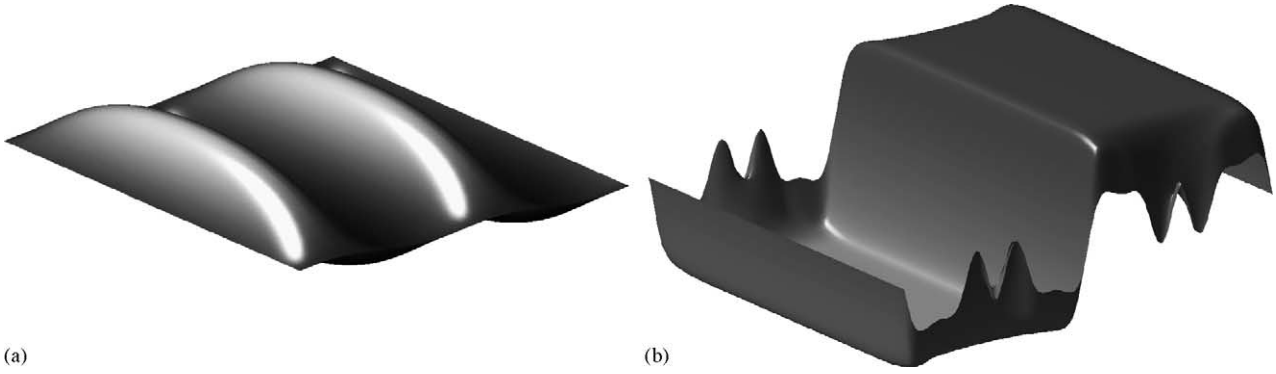

Fig. 2. Polarization profile (a) for soft domains ($2a_f = 700$ nm, $T = 0$) and (b) for hard domains ($2a_f = 100$ nm, $T = 0.7T_c$). The scales in different directions are not proportional.

ovskite materials) we assume that the ferroelectric layers have either natural or strain-induced c-oriented uniaxial symmetry.

2. Basic equations

The physics of ferroelectric state is described by the system of electrostatic equations [4,5]:

$$\mathrm{div}(\mathbf{E} + 4\pi\mathbf{P}) = 0, \qquad \mathrm{rot}\,\mathbf{E} = 0, \tag{1}$$

in which the polarization is related to the electric field by the "equation of state" $\mathbf{P} = \mathbf{P}(\mathbf{E})$. That for z-component of the spontaneous polarization $P = P_z^{(\mathrm{f})}$ is given by the nonlinear Ginzburg–Landau equation:

$$tP + P^3 - (\partial_z^2 + \partial_x^2)P = \frac{\varepsilon_\parallel}{4\pi} E_z^{(\mathrm{f})}, \tag{2}$$

The temperature t in (2) is expressed via the critical temperature of the bulk short-circuited sample T_{c0} as: $t = T/T_{c0} - 1$, polarization P is measured in units of the uniform bulk polarization P_0 at $T = 0$ and all the lengths are scaled in units of the coherence length ξ_0. The dimensionless parameter $\varepsilon_\parallel \gg 1$ in (2) is expressed via the Curie constant as $\varepsilon_\parallel = C/T_{c0}$. The transversal component $P_x^{(\mathrm{f})}$ of polarization in ferroelectric layer as well as polarization components $P_{x,z}^{(\mathrm{p})}$ in the paraelectric layers are linearly dependent on electric field:

$$P_x^{(\mathrm{f})} = \frac{\varepsilon_\perp - 1}{4\pi} E_x^{(\mathrm{f})}, \qquad P_{x,z}^{(\mathrm{p})} = \frac{\varepsilon_\mathrm{p} - 1}{4\pi} E_{x,z}^{(\mathrm{p})}. \tag{3}$$

For simplicity the Laplacian $\partial_z^2 + \partial_x^2$ in (2) and paraelectric susceptibility ε_p in (3) are assumed to be isotropic.

The electrostatic boundary conditions at the paraelectric–ferroelectric interfaces:

$$E_z^{(\mathrm{f})} - E_z^{(\mathrm{p})} = -4\pi(P_z^{(\mathrm{f})} - P_z^{(\mathrm{p})}), \qquad E_x^{(\mathrm{f})} = E_x^{(\mathrm{p})} \tag{4}$$

are completed by the interface condition for the spontaneous polarization:

$$\partial_z P = \lambda P, \tag{5}$$

where λ is the extrapolation length [6] that reflects the properties of the interface.

In terms of electrostatic potential $\varphi^{(\mathrm{f,p})}$: $E_{z,x}^{(\mathrm{f,p})} = -\partial_{z,x}\varphi^{(\mathrm{f,p})}$ Eqs. (1)–(5) are written as

- Paraelectric layer(s):

$$(\partial_z^2 + \partial_x^2)\varphi^{(p)} = 0. \tag{6}$$

- Ferroelectric layer(s):

$$4\pi\varepsilon_{\parallel}^{-1}[t - (\partial_z^2 + \partial_x^2) + P^2]P = -\partial_z\varphi^{(\mathrm{f})}, \tag{7}$$

$$(\partial_z^2 + \varepsilon_{\perp}\partial_x^2)\varphi^{(\mathrm{f})} = 4\pi\partial_z P. \tag{8}$$

- Paraelectric/ferroelectric interface:

$$\partial_z\varphi^{(\mathrm{f})} - \varepsilon_{\mathrm{p}}\partial_z\varphi^{(\mathrm{p})} = 4\pi P, \tag{9}$$

$$\varphi^{(\mathrm{f})} = \varphi^{(\mathrm{p})}, \qquad \partial_z P = \lambda P. \tag{10}$$

One more boundary condition for the paraelectric/electrode interface:

$$\varphi^{(\mathrm{p})} = 0 \tag{11}$$

corresponds to the geometry of ferroelectric layer embedded into short-circuited capacitor. This condition admits the periodic continuation of solution in z-direction that makes both the presented in Fig. 1 geometries mathematically equivalent.

To calculate the domain structure profile $P(x, z)$ we have solved Eqs. (6)–(11) numerically, assuming the antiperiodic distribution of polarization and potential in x-direction. Considering now the domain width d as variational parameter we find the equilibrium (most stable) structure, substituting solution $P(x, z)$ into the generating Euler functional, that for its extremals is simplified to

$$F = -\frac{1}{4}\int P^4 \mathrm{d}x\mathrm{d}z, \tag{12}$$

and minimizing it over d.

For numerical calculations we selected the typical for the displacive ferroelectrics material parameters: $\varepsilon_{\parallel} \simeq 500$, $\varepsilon_{\perp} \simeq 100$, $\varepsilon_{\mathrm{p}} \simeq 10$. The coherence length was estimated as the low-temperature domain wall half-width $\xi_0 \simeq 10\,\text{Å}$. The ferroelectric film thickness $2a_{\mathrm{f}}$ varied between 25 and 1000 nm, the paraelectric layer thickness a_{p} was always selected larger then characteristic domain width to keep the sample in the multi-domain regime. The surface factor λ in this study was neglected.

3. Results

Basing on Eqs. (6)–(11) we calculated numerically both the dependence of the domain structure period on temperature and the temperature evolution of the polarization profile.

Fig. 3a presents the temperature dependence of domain width d for the films having different thickness $2a_{\mathrm{f}}$. It appears that this parameter is almost temperature independent. Basing on scaling properties of Eqs. (6)–(11) we can present the dependence $\mathrm{d}(T)$ in the generalized Kittel form as

$$\mathrm{d}(T) = \sqrt{\gamma(T)(\varepsilon_{\perp}/\varepsilon_{\parallel})^{1/2}2a_{\mathrm{f}}} \tag{13}$$

where the weakly temperature-dependent numerical parameter $\gamma(T)$ can be calculated analytically in the limit cases of low temperatures (at $T = 0$ when $\varepsilon_{\mathrm{p}}^2 \ll \varepsilon_{\perp}\varepsilon_{\parallel}$), using the Kittel approximation [1–3,5], and in vicinity of T_{c} [4,5]:

$$\gamma(0) = \frac{2\sqrt{2}\,\pi^3}{21\zeta(3)} \simeq 3.53, \qquad \gamma(T_{\mathrm{c}}) = \pi \tag{14}$$

Since the period of domain texture is almost temperature independent, the contribution of domain wall motion to the temperature hysteresis of ferroelectric properties should be weak.

Discuss now the temperature evolution of polarization profile inside domains. Phase diagram of domain states in thin films is shown in Fig. 3b. The transition from paraelectric to ferroelectric phase occurs directly into the shown in Fig. 2a periodically modulated soft domain structure in which the

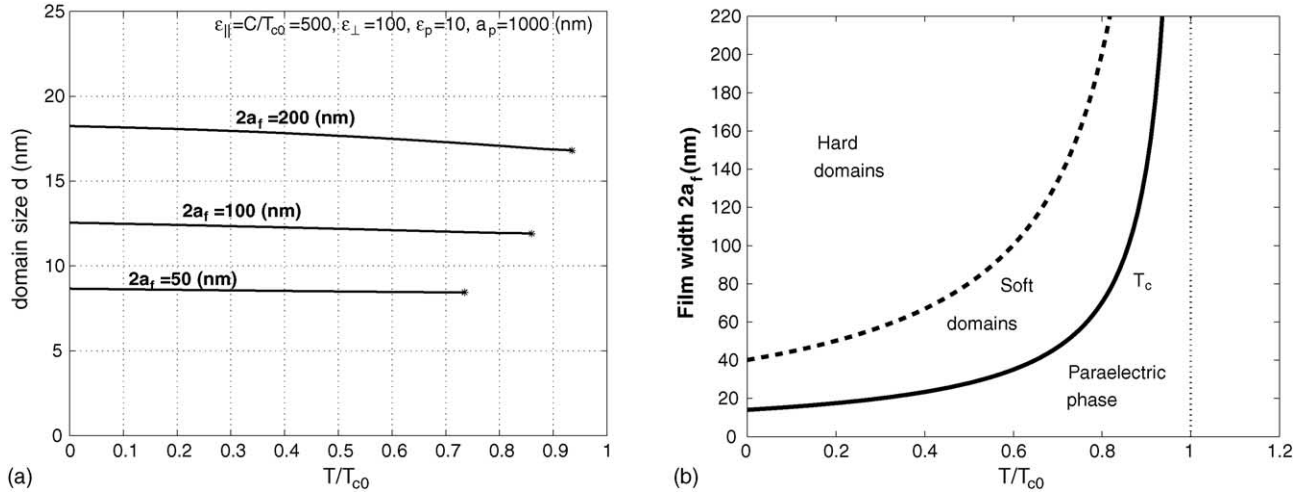

Fig. 3. (a) Temperature variation of equilibrium domain width d for films with different thickness. (b) Phase diagram of the domain states in thin film.

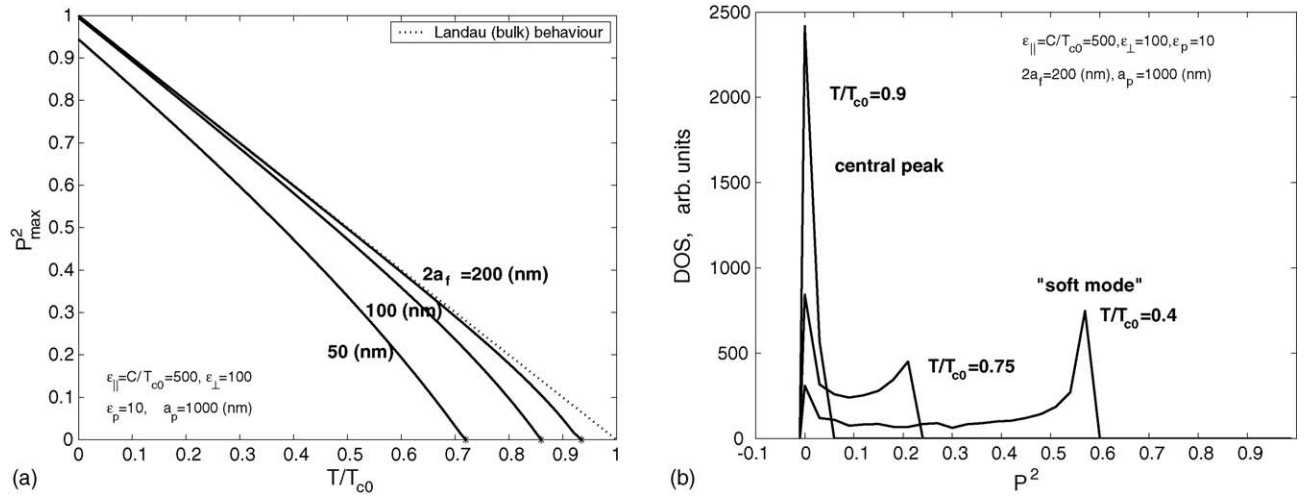

Fig. 4. (a) Temperature dependence of the square of polarization in center of domain P^2_{max} for films with different thickness $2a_f$. Dotted line shows the Landau-type behavior for the bulk mono-domain short-circuited sample. (b) Density of states of square of polarization P^2 for the domain structure in film of thickness $2a_f = 200$ nm at different temperature.

gradual polarization distribution is approximately written as [4]:

$$P(x, z) = P_{max}(T) \sin(\pi x/d) \cos(\pi z/2a_f). \quad (15)$$

Since creation of domain structure costs the gradient and depolarization field energy, the transition temperature T_c is reduced with respect to transition temperature of the bulk short circuited sample T_{c0} as [4,5]:

$$T_c \approx T_{c0} \left(1 - \sqrt{\frac{\varepsilon_\parallel}{\varepsilon_\perp}} \frac{\pi}{a_f}\right). \quad (16)$$

When temperature decreases below T_c the amplitude of polarization modulation P_{max} increases and, at the same time, the polarization profile in the domain centers becomes more flat. At lower temperatures the polarization profile inside domains becomes hard, as shown in Fig. 2b.

To study the crossover from soft to hard domains we plotted in Fig. 4a the temperature dependence of polarization square in the domain center $P^2_{max}(T)$. In the soft regime (in vicinity of transition) $P^2_{max}(T)$ follows the Landau-type behavior $\sim T - T_c$. In the hard-profile regime the temperature dependence again becomes linear but with the bulk transition temperature T_{c0} as the critical temperature parameter ($P^2_{max} \sim T - T_{c0}$). Therefore, the thermodynamics of the film with hard domains is the same as that of the bulk short-circuited sample and neither the surface-located depolarization field nor the thin domain walls play substantial role in it.

Meanwhile, the depolarization field plays the important role in the polarization profile close to the film surface. As follows from Fig. 2b, in the hard regime, it results both to considered in [7] surface polarization damping and to intervention of the small surface-located inversely polarized domains. This phenomenon, known as Landau–Lifshitz domain branching [2] was reproduced in our numerical calculations up to the second branching level. In the soft domains (Fig. 2a), polarization always vanishes on the film surface.

As follows from Fig. 3b, the crossover temperature between soft and hard domain states decreases with film thickness in the same way as T_c, i.e. inversely proportional to $2a_f$. The temperature interval of existence of soft domains becomes very large for the thin nanometric films and their physical properties can be governed by the highly nonuniform distribution of polarization across the sample.

The gradual polarization variation in soft domains can be visualized by experimental techniques testing the local distribution of polarization such as Raman and infrared spectroscopy, X-ray diffraction, ESR, etc. Fig. 4a shows the density of states (DOSs) of local values of polarization square P^2 at different temperatures. It appears that in vicinity of T_c the domain walls region pumps over a DOS from the "soft mode" peak at P^2_{max} into the central peak at $P^2 = 0$ that can result in misinterpretation of soft-mode spectroscopy measurements.

To conclude we have shown that properties of ferroelectric nanometric thin films are substantially governed by the gradual polarization distribution in soft domain texture. At the same time, the width of ferroelectric domains is not sensitive to polarization distribution and is almost temperature independent.

Acknowledgement

This work was supported by region of Picardy, France.

References

[1] C. Kittel, Phys. Rev. 70 (1946) 965.

[2] L.D. Landau, E.M. Lifshitz, Electrodynamics of Continuous Media, Elsevier, New York, 1985.
[3] A.M. Bratkovsky, A.P. Levanuk, Phys. Rev. Lett. 84 (2000) 3177.
[4] E.V. Chensky, V.V. Tarasenko, Sov. Phys. JETP 56 (1982) 618 [Zh. Eksp. Teor. Fiz. 83 (1982) 1089].
[5] V.A. Stephanovich, I.A. Luk'yanchuk, M.G. Karkut, Phys. Rev. Lett. 94 (2005) 047601.
[6] R. Kretschmer, K. Binder, Phys. Rev. B20 (1979) 1065.
[7] Y.G. Wang, W.L. Zhong, P.L. Zhang, Phys. Rev. 51 (1995) 5311.